Patterning and photoluminescence of CdS nanocrystallites on silk fibroin fiber

ARTICLE *in* JOURNAL OF NANOPARTICLE RESEARCH · JANUARY 2010

Impact Factor: 2.18 · DOI: 10.1007/s11051-009-9622-1

J Nanopart Res (2010) 12:347–356
DOI 10.1007/s11051-009-9622-1

RESEARCH PAPER

Patterning and photoluminescence of CdS nanocrystallites on silk fibroin fiber

Jie Han · Huilan Su · Qun Dong · Di Zhang · Xiaoxiao Ma · Chunfu Zhang

Received: 22 November 2008 / Accepted: 6 March 2009 / Published online: 26 March 2009

Abstract CdS nanocrystallites could be formed and assembled into nanoparticle strings and hexagons on natural silk fibroin fiber (SFF) through a room-temperature bio-inspired process. Herein, the biomaterial SFF served as reactive substrate, not only provides the in situ formation sites for CdS nanocrystallites, but also directs the arrangement of nanocrystalline CdS simultaneously. The photoluminescence (PL) of the resulting nanocomposites CdS/SFF is investigated extensively. The PL peaks observed from CdS nanoparticle strings are similar to those of separate CdS nanoparticles, corresponding to the band-edge emission of their individual building blocks (QD-CdS). Moreover, CdS nanoparticle hexagons perform a red-shifted and broadened emission peak.

Keywords Chalcogenides · Nanostructures · Chemical synthesis · Photoluminescence spectroscopy · Bio-inspired · Quantum dots

Introduction

The bottom-up synthesis of well-established quantum dots (QD) into some special nanostructures for future nanodevices presently receives increasing research interest. Various organized structures of semiconductor nanoparticles, including nanocomposite films (Zimnitsky et al. 2007), helical arrays (Zhou et al. 2006), aerogel networks (Arachchige and Brock 2006), superlattices (Murray et al. 2001), necklaces (Zhang et al. 2006; Xue et al. 2004), rings (Liu and Zeng 2005), alignments (Berman and Charych 1999; Berman et al. 2003; Cavallini et al. 2007) and so on, have been fabricated and presented valuable performances related to their special nanoarchitectures. Thereinto, Vossmeyer et al. observed a redshift of the first electronic transition on QD compact layers compared to the same QD dispersed in solution (Vossmeyer et al. 1994). Also, Bawendi group prepared a very fine crystalline superstructure of semiconductor nanoparticles and found similar red-shifted optical properties (Murray et al. 1995; Kagan et al. 1996; Döllefeld et al. 2002).

The in situ bottom-up synthesis involving a subtle medium is thought to be a promising route

Electronic supplementary material The online version of this article (doi:10.1007/s11051-009-9622-1) contains supplementary material, which is available to authorized users.

J. Han · H. Su (✉) · Q. Dong · D. Zhang (✉) · X. Ma
State Key Laboratory of Metal Matrix Composites, Shanghai Jiaotong University, Shanghai 200240, China
e-mail: hlsu@sjtu.edu.cn

D. Zhang
e-mail: zhangdi@sjtu.edu.cn

C. Zhang
Med-X Research Institute, Shanghai Jiaotong University, Shanghai 200240, China

to semiconductor nanoarchitectures. Functionalized dendronized polymers, organogel fibers (Zhang et al. 2006; Xue et al. 2004), functionalized glycolipid nanotubes (Zhou et al. 2006), peptide-amphiphile (Sone and Stupp 2004) and modified carbon nanotubes (Li et al. 2006) have already been chosen as such media to serve as both the in situ synthesis nanoreactors and the assembling assistants of inorganic nanoparticles. Yet the organized hybrid nanoarchitectures are usually steady only in solution, which limits their applications (Wang and Moffitt 2005). Considering the outstanding photoluminescence of QD and their potential applications in various solid state nanodevices, it is necessary to create new synthesis techniques for well-organized nanostructures on some solid substrates.

Natural silk fibroin fiber (SFF) extracted from the silkworm *Bomboyx mori* cocoons is commercially available material that has been widely used in textile production and biomedical fields for its impressive mechanical properties as well as biocompatibility. SFF contains at least two major fibroin proteins that are connected by a disulfide link, light (25 kDa) and heavy chains (350 kDa) (Kim et al. 2004; Chen et al. 2003). During the spinning process in silkworm's gland, the shear and elongational stress acting on the fibroin solution cause the formation of antiparallel β sheet crystalline regions. And elongational flow orients the fibroin chains, converting the liquid into fiber constructed by thousands of parallel fibrils (Jin and Kaplan 2003; Ayutsede et al. 2006). Since proteins are capable to bind inorganic nanoparticles and even some enchanting interactions between the two parts have been observed (Niemeyer 2003), the unique fibril structures along with the richness of amino acids components make SFF attractive substrate for ordered nanostructures constructed by inorganic nanoparticles. In addition, considering the biocompatibility of natural SFF, as-prepared hybrids might have potential applications in bio-related fields. Moreover, our previous studies have proven that SFF is the effective biotemplate to deposit silver nanoclusters on the surface (Dong et al. 2005).

CdS is a typical semiconductor with the direct bandgap near 2.4 eV for bulk material. By controlling their size and surface functionality, CdS nanoparticles display tunable photoluminescence that span the visible spectrum, having potential applications in biolabel, photonics, sensor, ion-probe, and so on (Sapra et al. 2001; Du et al. 2002; Chen and Rosenzweig 2002). Moreover, the organized nanostructures are also found to have great influence on their properties. Y. Lin et al. reported the interaction of the photonic stop band with the photoluminescence from the CdS nanocrystals in a specific self-organized photonic crystal, whose building blocks polymer microspheres are surrounded by CdS nanocrystal satellites (Lin et al. 2002). Efforts are still needed to investigate the controlled synthesis and assembly of CdS nanoparticles with tunable properties, in the hope of fabricating novel nanodevices for future applications.

In this work, a bio-inspired in situ synthesis is applied to fabricate QD-CdS nanostructures with different patterns on SFF. Briefly, SFF are sequentially immersed into Cd-precursor and S-precursor solutions, turning the fibers from white to yellow instantly. The synthesis conditions are varied in order to control the particle sizes and corresponding arranged patterns of CdS nanoparticles, as well as to investigate their photoluminescence.

Experimental

Cocoons were taken directly from the cultivating boxes of *B. mori* silkworm, and treated in 20 mM Na_2CO_3 solution at 110 °C for about 1 h to remove the gummy binding protein sericin to obtain SFF. All these chemicals $CdCl_2 \cdot 2.5H_2O$, $NH_3 \cdot H_2O$, $Na_2S \cdot 9H_2O$, Na_2CO_3, $CaCl_2$, and ethanol with analytical grade were purchased from Shanghai Chemical Company and were used without further purification. Cd-Precursor was prepared as follows: 25 mL 0.05 M $CdCl_2$ solution was mixed with 20 mL 5% ammonia, then diluted to 100 mL (final solution pH = 11). S-Precursor was 0.0625–6.25 mM Na_2S solution.

A certain amount of SFF was first immersed into Cd-precursor for 1–2 days, then taken out and rinsed with deionized water for several times to obtain Cd-SFF hybrid complexes. Subsequently, the Cd-SFF hybrids were immersed into S-precursor and turned from white to yellow immediately. The yellow fiber product was taken out and rinsed with deionized water, and finally dried in vacuum at room temperature for further characterization. The synthesis conditions are present in detail in Table 1.

The samples for UV–vis, TEM, HRTEM, and PL observation (mentioned as "QD-CdS/SFF sample ×

Table 1 Synthesis conditions and samples' features

Sample	Immersing time in $CdCl_2$ solution (h)	Concentration of Na_2S solution (mM)	Immersing time in Na_2S solution	Arranged patterns[a]	λ^b_{edge} (nm)	E^b_{edge} (eV)	Diameter of QD-CdS[b] (nm)
I	24	0.0625	30 s	–	485	2.56	5.3
II	24	0.313	30 min	Strings	507	2.45	7.2
III	24	First 0.313 mM 30 min then 6.25 mM 15 s		Strings and hexagons	511	2.43	7.9
IV	48	0.313	24 h	Strings and hexagons	511	2.43	7.9
V	48	6.25	15 s	–	439	2.83	3.8
VI	48	6.25	24 h	Strings and hexagons	465	2.67	4.4
VII	48	6.25	48 h	–	–	–	–

[a] Arranged patterns of QD-CdS assemblies are observed by FESEM/TEM

[b] λ_{edge}, E_{edge}, and diameter of QD-CdS are calculated from the UV–vis spectra

Data at "–" were not collected

dispersed in $CaCl_2$ solution" in this article) were prepared as below: a certain amount of yellow product was immersed in a ternary solution [$CaCl_2$:H_2O:-C_2H_5OH = 1:8:2 (mole ratio)] at 50 °C for several hours to dissolve SFF and disperse CdS assemblies in silk fibroin (SF) solution. UV–vis spectra were performed on Shanghai Spectrum Instruments Co., LTD 752PC, taking corresponding SF solutions without CdS as the reference (the concentrations of SF are the same). FESEM images were obtained on a FEI Sirion 200 field emission gun scanning electron microscope with samples pre-sputtered Au on their surface to prevent charging during observation. TEM measurements were operated on a JEOL-2010 transmission electron microscope under an acceleration voltage of 200 kV. HRTEM measurements were operated on a JEM-2100F instrument under an acceleration voltage of 200 kV. PL (photoluminescence) spectra were taken on Perkin-Elmer LS 55 with both solid yellow samples and the samples dispersed in $CaCl_2$ solution (excitation wavelength: 365 nm, excitation slit: 10 nm, emission slit: 10 nm).

Results and discussion

Size-tunable CdS nanoparticles on SFF

The original SFF was immersed into the Cd-precursor, washed several times by distilled water, and immersed into Na_2S solution to turn yellow immediately. The yellow color might be attributed to the formation of CdS. Herein, UV–vis absorption spectra were taken to investigate the yellow products. Since bulk CdS has the band gap energy around 2.4 eV at room temperature, QD-CdS nanoparticles (the diameter ≤6 nm) have the absorption threshold shorter than 515 nm (Henglein 1989). As shown in Fig. 1, the absorption edges of the UV–vis spectra appear around 500 nm, indicating that the yellow products might be QD-CdS. Furthermore, the direct band gap energy and the diameter of QD-CdS could be obtained by applying the following equations (see Supplementary Material) (Nag 2000; Brus 1984; Bawendi et al. 1990). Table 1 describes the synthesis conditions and corresponding features of different samples.

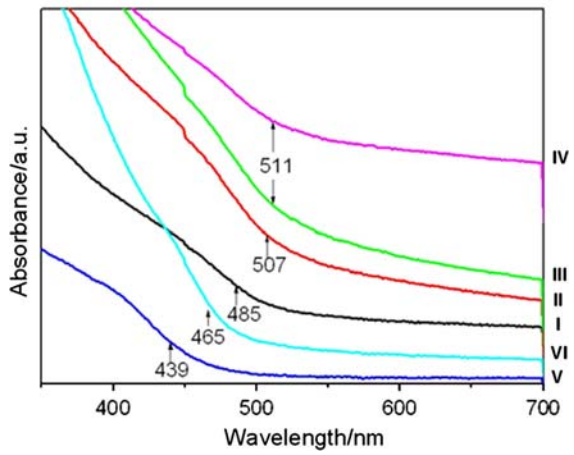

Fig. 1 UV–vis absorption spectra of sample I–VI dispersed in $CaCl_2$ solution. (reference: corresponding silk fibroin (SF) dispersed in $CaCl_2$ solution). λ_{edge} calculated from the spectra are indicated by arrows. (The plots are shifted vertically for clarity.)

$$\alpha h\nu = A\left(h\nu - E_g\right)^{1/2} \quad (1)$$

$$E = E_{\text{bulk}} + \frac{\hbar^2\pi^2}{2R^2}\left[\frac{1}{m_e} + \frac{1}{m_h}\right] - \frac{1.786e^2}{\varepsilon R} \quad (2)$$

Besides, the cross-sections of sample II were investigated by HRTEM observation, which elucidates the feature of QD-CdS on undissolved fibers and proves the reliability of the diameters evaluated from the UV–vis spectra (see Supplementary Material).

By prolonging the immersing time in Na_2S solution (sample V → VI), the absorption edge is shifted to longer wavelength, indicating the increase of the particle size. When the concentration of Na_2S solution is increased, the absorption edge presents a blue-shift, implying the formation of smaller nanoparticles (sample IV→VI). Therefore, under the assistance of biotemplate SFF, the size of QD-CdS formed on SFF is proportional to the immersing time and inverse proportional to the concentration of Na_2S solution.

Different arrangement of size-tunable QD-CdS on SFF

The samples display different organized patterns, as listed in Table 1. Sample II contains only strings pattern, while samples III, IV, and VI contain both strings and hexagons patterns. Herein, samples II, IV and VI were prepared by the sequential immersion into Cd-precursor and S-precursor, with different precursor concentration and immersing time. While sample III was prepared by immersing sample II into Na_2S solution with higher concentration (6.25 mM) for 15 s.

Original SFF displays a relatively smooth surface after gold-sputtering treatment (Fig. 2a), yet its parallel fibrils are still distinguishable under the higher magnification (indicated by a double arrow in Fig. 2c). Figure 2b and d represent as-prepared yellow QD-CdS/SFF (sample II). It should be mentioned that Fig. 2b displays similar smooth appearance to Fig. 2a, which demonstrates the small size and homogeneous distribution of as-prepared QD-CdS on SFF. Besides, the QD-CdS trace the original parallel fibrils and perform string-like arrangement pattern on the surface of sample II. Thus the orientation of QD-CdS strings is consistent with the axis of biosubstrate SFF (indicated by a double arrow in Fig. 2d).

These CdS nanoparticle strings could be further investigated by TEM observation. Sample II was treated in $CaCl_2$ solution to dissolve SFF. Figure 2e clearly shows the strings pattern of QD-CdS arrangement. However, a careful look reveals some loosely connected QD-CdS along with these nanoparticle strings (Fig. 2f). It should be caused by the slightly over-dissolution of SFF during the TEM sample preparation, and indicates the importance of SFF on connecting QD-CdS to nanoparticle strings. The size of QD-CdS estimated from Fig. 2f is 6–8 nm, which is in agreement with the results from UV–vis spectra. SAED gives the evidence of the inorganic components among the string-like structures, although the diffraction signals are weak due to the limited amount of particles selected. Moreover, they can be indexed to (101), (110), and (103) according to the CdS hexagonal (greenockite) structure reported in JCPDS cards 41-1049 as presented in the inset. Therefore, hexagonal QD-CdS have been successfully synthesized and arranged into nanoparticle strings on the biosubstrate SFF.

QD-CdS/SFF sample VI (Fig. 3a, c, and e), sample III (Fig. 3b and d) and sample IV (Fig. 3f) display both strings and hexagons' patterns on the fiber surface. HRTEM images of such hexagons are shown in Fig. 3e, while higher magnification images are unavailable due to the thickness of the hexagons. However, a piece of thin broken hexagon of sample IV (Fig. 3f) makes it possible to observe them in detail. It is obvious that the hexagons are QD-CdS assemblies, and the inset in Fig. 3f displays a single QD-CdS nanoparticle inside the hexagon with lattice fringes correspond to (110) planes of QD-CdS. Thus, the grey area in Fig. 3e should comprise single QD-CdS particles. And the larger dark particles should be small aggregations of QD-CdS, according to the small size of CdS particles estimated from the UV–vis results. Similar hexagons are also obtained on sample III (Fig. 3d), which was prepared by further treatment of sample II on only which nanoparticle strings could be observed. However, the size of the building blocks (QD-CdS) of both strings and hexagons on sample III is larger than that on sample VI, which is predicted by UV–vis results. So the larger building blocks could be directly seen in Fig. 3d, and

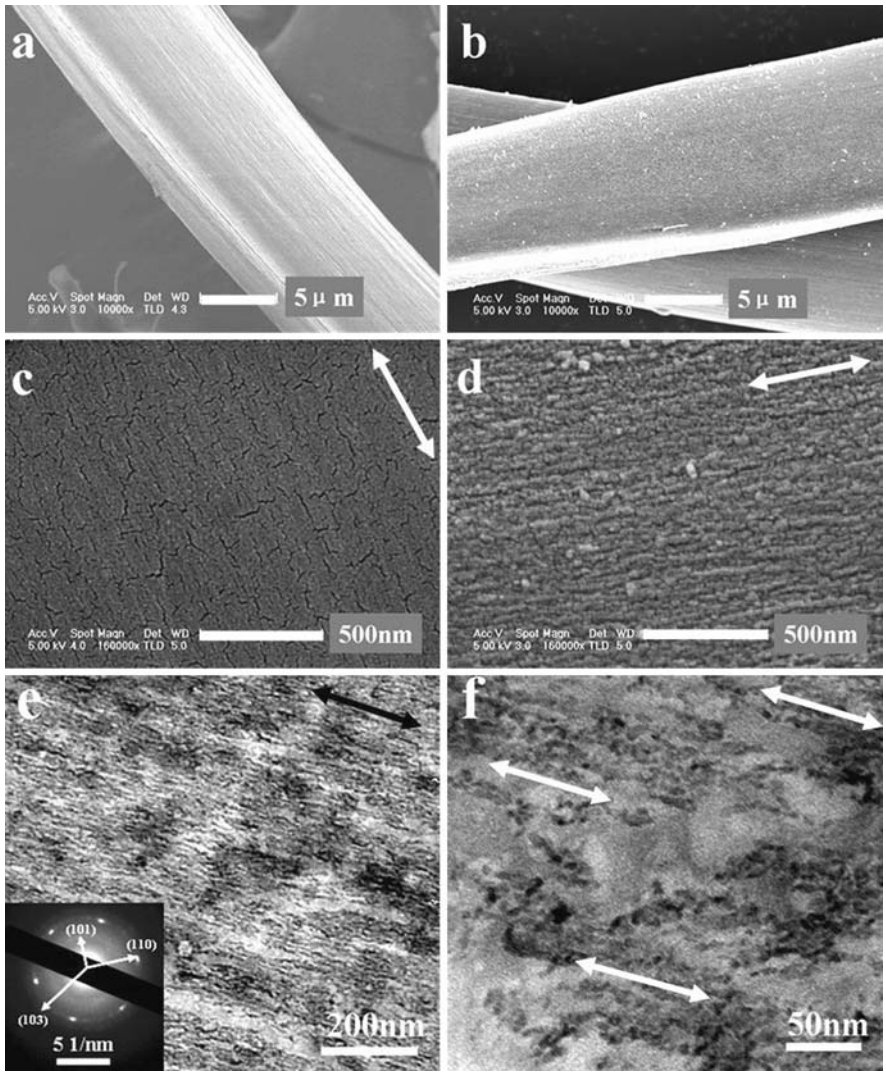

Fig. 2 FESEM images of original SFF (**a** and **c**) and QD-CdS/SFF sample II (**b** and **d**), as well as TEM images of QD-CdS/SFF sample II dispersed in $CaCl_2$ solution (**e** and **f**). Double arrows indicate the orientation of parallel fibrils (**c**), the axis of biosubstrate SFF (**d**) and the orientation of CdS nanoparticle strings (**e** and **f**). Inset in **e** shows respective SAED patterns of the certain area

the hexagons are observed to be assembled by QD-CdS.

In Fig. 3b, some hexagonal holes appear among the CdS nanoparticle strings on QD-CdS/SFF sample III and there are only a few CdS nanoparticles loosely dispersed on the smooth SFF surface inside these holes. Since QD-CdS/SFF sample II contains only continuous nanoparticle strings, these hexagonal disruptions on sample III should be owing to the missing of some existent QD-CdS during the additional treatment of sample II in 6.25 mM Na_2S solution. Moreover, considering the CdS nanoparticle hexagons (Fig. 3d) and the holes caused by lost QD-CdS (Fig. 3b) have similar hexagonal shape for the same sample, the lost QD-CdS are supposed to aggregate into nanoparticle hexagons before leaving SFF. That is, by further treating sample II into 6.25 mM Na_2S solution, some QD-CdS could easily pattern into nanoparticle hexagons (as fast as 15 s). So the building blocks of the hexagons are most likely root from QD-CdS that arranged for string patterns. Besides, hexagons also occur under the condition of relatively long immersing time (24 h) in 0.313 mM Na_2S solution (sample IV, Fig. 3f). It is reasonable to suggest that the relatively high concentration Na_2S solution or the long time immersing in Na_2S solution slightly dissolves SFF to some bioresidues, which further connect the preformed QD-CdS and rearrange them into hexagonal aggregation patterns (Scheme 1).

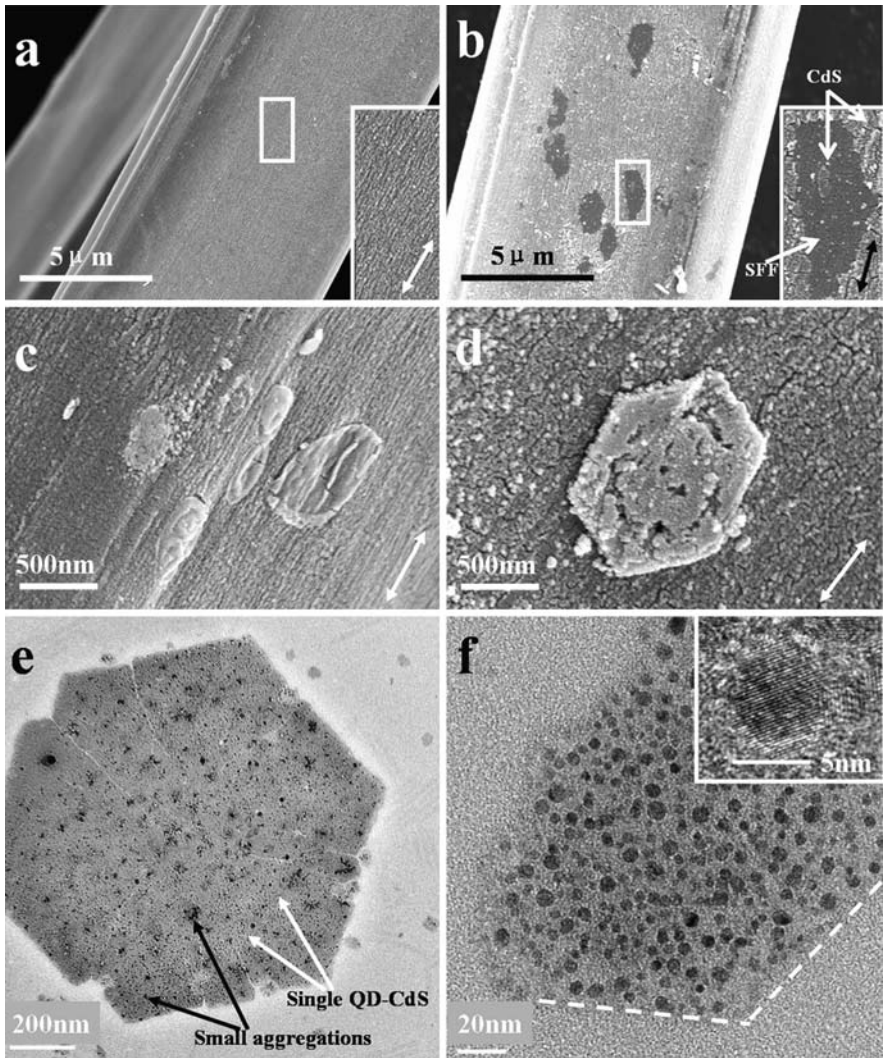

Fig. 3 FESEM images of QD-CdS/SFF sample VI (**a** and **c**) and sample III (**b** and **d**), as well as HRTEM images of the nanoparticle hexagons and broken hexagons obtained by dispersing QD-CdS/SFF sample VI (**e**) and sample IV (**f**) in $CaCl_2$ solution. *Double arrows* in **a**–**d** indicate the fiber axis. Insets in **a** and **b** show images of the corresponding rectangular areas under higher magnification. **f** shows a single QD-CdS in the hexagons

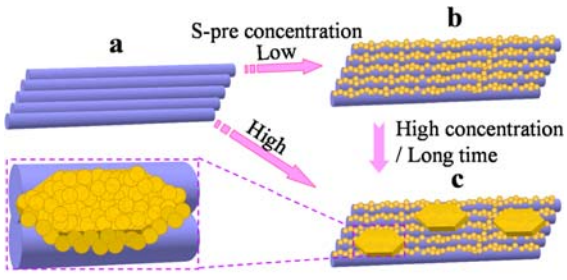

Scheme 1 Illustration of the different arrangement of nano-CdS on SFF under different conditions

Photoluminescence properties of the assembled structures

The photoluminescence (PL) spectra of the two types of QD-CdS/SFF samples were measured. As shown in Fig. 4, the sample II that contains CdS nanoparticle strings has a broad PL peak around 500 nm, which is close to the absorption edge 507 nm and should be considered as the band-edge emission of individual QD-CdS (Henglein 1989; Wang and Moffitt 2004; Jaiswal et al. 2003). The broad peak suggests a broad-size distribution of QD-CdS in this sample. In addition, the PL band-edge emission from the same QD-CdS dispersed in SF solution is around 500 nm (see Supplementary Material) too. So the PL

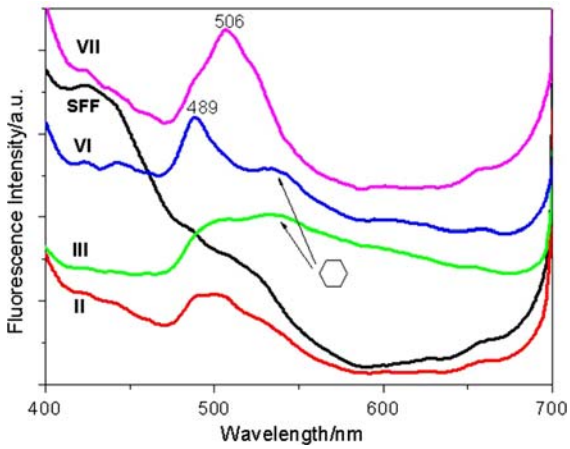

Fig. 4 PL spectra of original SFF and QD-CdS/SFF sample II, III, VI, VII. (excitation wavelength: 365 nm. The plots are shifted vertically for clarity.)

properties of as-prepared CdS nanoparticle strings are similar to those of separate/individual QD-CdS.

QD-CdS/SFF sample III contains both CdS nanoparticle strings and hexagons, with the building blocks slightly larger than that of sample II according to previous UV–vis results as well as PL spectra of their separate building blocks (see Supplementary Material, Fig. S3 and S4). Therefore, the band-edge emission from the individual building blocks of both assembled structures in sample III should be predicted around and slightly red-shifted from 500 nm (Brus 1984; Bawendi et al. 1990). However, the PL spectrum of sample III presents an additional broad peak around 530 nm in comparison with that of sample II, besides the predicted red-shifted band-edge emission (around 500 nm) from CdS nanoparticle strings. This additional peak might come from nanoparticle hexagons. As concerning sample III, the PL properties of individual building blocks (corresponding to the nanoparticle strings, around 500 nm) and nanoparticle hexagons (around 530 nm) are present, so it is obvious that the emission peak of nanoparticle hexagons is broadened and red-shifted from the peak of corresponding individual building blocks. In Figure 4, VI displays the band-edge emission from CdS nanoparticle strings at shorter wavelength, while other features are the same as III in Fig. 4, which is in great agreement with the previous observations that sample VI contains similar aggregation patterns to sample III but is constructed by smaller building blocks. However, in the case of sample VII, the band-edge emission from nanoparticle strings appears so close to the PL peak of nanoparticle hexagons that only a complex peak is observed. Therefore, as-prepared CdS nanoparticle hexagons present red-shifted and broadened PL spectra when compared with separate/individual QD-CdS.

Figure 5 displays the PL spectra of separate QD-CdS dispersed in SF solution. Double peaks in Fig. 5II and III are fitted by multi-peaks fitting method (Lorentzian mode, see Supplementary Material). For QD-CdS/SFF sample II and III, the peaks at longer wavelength represent the band-edge emission of QD-CdS with a slight size effect (Jin and Kaplan 2003; Ayutsede et al. 2006). In the case of sample VI, QD-CdS band-edge emission should appear at shorter wavelength according to the smaller size of the particles. Thus, sample VI emits an integrated band that combines the emission from QD-CdS and SF solution. QD-CdS have two characteristic PL peaks, corresponding to band-edge emission around 500 nm, and deep trap/surface state emission (broad band between 550 and 800 nm) (Henglein 1989; Wang and Moffitt 2004; Jaiswal et al. 2003). In Fig. 5II only band-edge emission is observed, indicating the few defects in the as-separated building blocks of nanoparticle strings. However, both band-edge emission and deep trap/surface state emission exist in Fig. 5III and Fig. 5VI, revealing defects in the separated QD-CdS from the two samples containing nanoparticle hexagons. These defects should come from the separation process of nanoparticle hexagons in $CaCl_2$

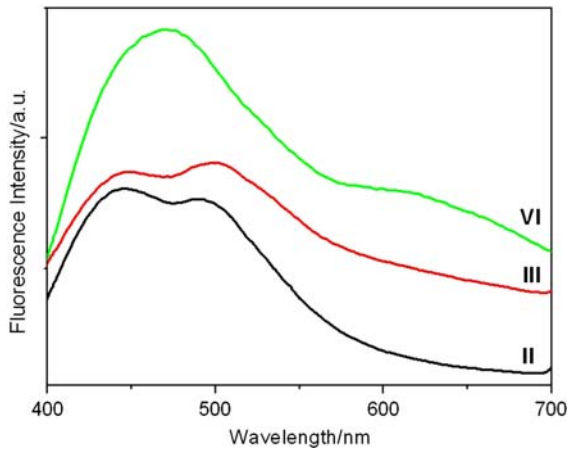

Fig. 5 PL spectra of QD-CdS/SFF sample II, III, and VI dispersed in $CaCl_2$ solution. (excitation wavelength: 365 nm. The plots are shifted vertically for clarity.)

solution, now that similar deep trap/surface state emission is absent in Fig. 5II, 4III and 4VI. It should be mentioned that the peaks in Fig. 4 with very low intensities between 600 and 700 nm in the PL curves of QD-CdS/SFF sample III and VI also exist in the curves of original SFF and other QD-CdS/SFF samples, which should be considered as the SFF PL emission instead of the QD-CdS deep trap/surface state emission. After all, well-dispersed building blocks of nanoparticle hexagons have both band-edge emission and deep trap/surface state emission, while dispersed building blocks of nanoparticle strings present only band-edge emission.

Furthermore, different amounts of QD-CdS/SFF sample V were dispersed in the same volume of $CaCl_2$ solution to investigate the PL properties, in the hope of revealing the correlation of SFF and QD-CdS in the nanoparticle hexagons. As-prepared solution with high sample concentration was named as Sample V (high) and that with low sample concentration was named as Sample V (low). Sample V (low) performs similar PL spectrum to Sample VI as shown in Fig. 5, owing to the interlapped PL peaks of SF solution and separate QD-CdS. However, by dispersing sample V in $CaCl_2$ solution with high ratio, the PL spectrum changes obviously for the emergence of the emission around 530 nm, representing QD-CdS nanoparticle hexagons as revealed in Fig. 4. It is proposed that some nanoparticle hexagons remain undispersed in this case. In addition, the dissolution of SFF is insufficient if a large amount of sample is added to $CaCl_2$ solution. So the undispersed nanoparticle hexagons are possibly connected by undissolved SFF. Figure 6VII (late) and VII (early) provide additional evidence for the hypothesis. Sample VII was dispersed in $CaCl_2$ solution with high concentration. According to Fig. 6VII (early) that measured just after the dispersing, the 530 nm emission from nanoparticle hexagons is discernable but the surface states emission is hardly observed due to the small amount of dispersed nanoparticle hexagons. However, after a long-time storage for about 2 months, the PL spectrum was measured again (Fig. 6 VII (late)) and the 530 nm emission disappears along with an enhancement of the surface states emission (broad band between 550 and 800 nm). It suggests the slow dispersion of nanoparticle hexagons, which should be due to the slow dissolution of SFF that connect QD-CdS. Therefore, SFF plays important roles in connecting QD-CdS in these nanoparticle hexagons.

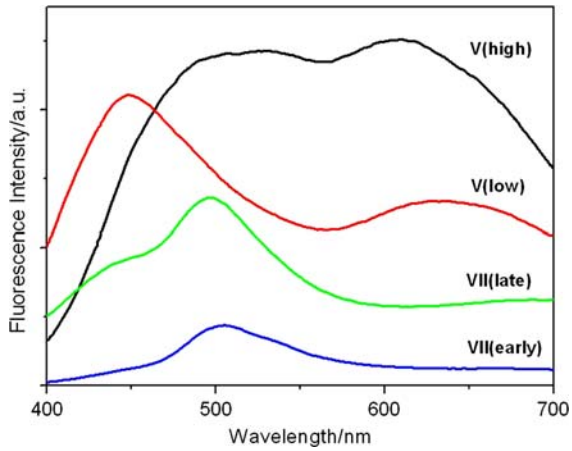

Fig. 6 PL spectra of different amounts of QD-CdS/SFF sample V dispersed in the same volume of $CaCl_2$ solution: as-prepared solution with high concentration (sample V (high)) and that with low concentration (sample V (low)). PL spectra of QD-CdS/SFF sample VII dispersed in $CaCl_2$ solution, which were measured just after the dispersing (VII (early)), as well as after 2 months storage (VII (late)). (excitation wavelength: 365 nm. The plots are shifted vertically for clarity.)

Based on the above analyses, it can be believed that the PL properties of CdS nanoparticle strings are the same as that of separate QD-CdS, the PL emission of CdS nanoparticle hexagons is red-shifted and broadened from that of separate QD-CdS, as well as SFF plays important roles in the assembly of QD-CdS into hexagons pattern.

Conclusion

CdS nanoparticle strings and hexagons have been fabricated through a bio-inspired in situ synthesis route, introducing natural SFF as the substrate, the in situ synthesis nanoreactor for QD-CdS formation as well as the assembling assistant for arranging QD-CdS into specific patterns. The size of the building blocks (hexagonal QD-CdS) of different patterns is proportional to the immersing time and inverse proportional to the concentration of Na_2S solution. CdS nanoparticle strings are commonly obtained among the samples, tracing the parallel fibrils on SFF. CdS nanoparticle hexagons appear when the concentration of Na_2S solution is relatively high (e.g., 6.25 mM) or the immersing time in Na_2S solution is relatively long (e.g., 24 h), and are

believed to be assembled from preformed CdS nanoparticle strings. The two patterns of CdS nanoparticles present different photoluminescence. The PL emission of CdS nanoparticle strings are similar to that of separate QD-CdS, corresponding to the band-edge emission. While the nanoparticle hexagons display red-shifted and broadened PL emission compared with that of separate QD-CdS. The solid and biocompatible substrate SFF makes nanostructured CdS more convenient to apply to more fields.

Supplementary material

Replotted UV–vis absorption spectra; HRTEM image of cross-sectioned sample II; PL spectra of QD-CdS/SFF sample II and III dispersed in $CaCl_2$ solution and the corresponding fitting curves.

Acknowledgements Financial supports from the national Science Foundations of China (no. 50671065, no. 30870682) and the Major Fundamental Research Project of Shanghai Science and Technology Committee (no. 07DJ14001, no. 08ZR1411100) are gratefully acknowledged. The authors also thank SJTU Instrument Analysis Center for the measurements.

References

Arachchige IU, Brock SL (2006) Sol-gel assembly of CdSe nanoparticles to form porous aerogel networks. J Am Chem Soc 128:7964–7971. doi:10.1021/ja061561e

Ayutsede J, Gandhi M, Sukigara S, Ye HH, Hsu CM, Gogotsi Y, Ko F (2006) Carbon nanotube reinforced Bombyx mori silk nanofibers by the electrospinning process. Biomacromolecules 7:208–214. doi:10.1021/bm0505888

Bawendi MG, Steigerwald ML, Brus LE (1990) The quantum mechanics of larger semiconductor clusters ("quantum dots"). Annu Rev Phys Chem 41:477–496

Berman A, Charych D (1999) Uniaxial alignment of cadmium sulfide on polymerized films: electron microscopy and diffraction study. Adv Mater 11:296–300. doi:10.1002/(SICI)1521-4095(199903)11:4<296::AID-ADMA296>3.0.CO;2-F

Berman A, Belman N, Golan Y (2003) Controlled deposition of oriented PbS nanocrystals on ultrathin polydiacetylene templates at the air-solution interface. Langmuir 19:10962–10966. doi:10.1021/la035419s

Brus LE (1984) Electron-electron and electron-hole interactions in small semiconductor crystallites: the size dependence of the lowest excited electronic state. J Chem Phys 80:4403–4409. doi:10.1063/1.447218

Cavallini M, Facchini M, Albonetti C, Biscarini F, Innocenti M, Loglio F, Salvietti E, Pezzatini G, Foresti ML (2007) Two-dimensional self-organization of CdS ultra thin films by confined electrochemical atomic layer epitaxy growth. J Phys Chem C 111:1061–1064. doi:10.1021/jp0668908

Chen YF, Rosenzweig Z (2002) Luminescent CdS quantum dots as selective ion probes. Anal Chem 74:5132–5138. doi:10.1021/ac0258251

Chen JS, Lu H, Richmond J, Kaplan DL (2003) Silk-based biomaterials. Biomaterials 24:401–416. doi:10.1016/S0142-9612(02)00353-8

Döllefeld H, Weller H, Eychmüller A (2002) Semiconductor nanocrystal assemblies: experimental pitfalls and a simple model of particle-particle interaction. J Phys Chem B 106:5604–5608. doi:10.1021/jp013234t

Dong Q, Su HL, Zhang D (2005) In situ depositing silver nanoclusters on silk fibroin fibers supports by a novel biotemplate redox technique at room temperature. J Phys Chem B 109:17429–17434. doi:10.1021/jp052826z

Du H, Xu GQ, Chin WS (2002) Synthesis, characterization, and nonlinear optical properties of hybridized CdS-polystyrene nanocomposites. Chem Mater 14:4473–4479. doi:10.1021/cm010622z

Henglein A (1989) Small-particle research: physicochemical properties of extremely small colloidal metal and semiconductor particles. Chem Rev 89:1861–1873. doi:10.1021/cr00098a010

Jaiswal JK, Mattoussi H, Mauro JM, Simon SM (2003) Long-term multiple color imaging of live cells using quantum dot bioconjugates. Nature Biotechnol 21:41–57

Jin HJ, Kaplan DL (2003) Mechanism of silk processing in insects and spiders. Nature 424:1057–1061. doi:10.1038/nature01809

Kagan CR, Murray CB, Bawendi MG (1996) Long-range resonance transfer of electronic excitations in close-packed CdSe quantum-dot solids. Phys Rev B 54:8633–8643. doi:10.1103/PhysRevB.54.8633

Kim UJ, Park JY, Li CM, Jin HJ, Valluzzi R, Kaplan DL (2004) Structure and properties of silk hydrogels. Biomacromolecules 5:786–792. doi:10.1021/bm0345460

Li CS, Tang YP, Yao KF, Zhou F, Ma Q, Lin H, Tao MS, Liang J (2006) Decoration of multiwall nanotubes with cadmium sulfide nanoparticles. Carbon 44:2021–2026. doi:10.1016/j.carbon.2006.01.033

Lin Y, Zhang J, Sargent EH, Kumacheva E (2002) Photonic pseudo-gap-based modification of photoluminescence from CdS nanocrystal satellites around polymer microspheres in a photonic crystal. Appl Phys Lett 81:3134–3136. doi:10.1063/1.1515881

Liu B, Zeng HC (2005) Semiconductor rings fabricated by self-assembly of nanocrystals. J Am Chem Soc 127:18262–18268. doi:10.1021/ja055734w

Murray CB, Kagan CR, Bawendi MG (1995) Self-organization of CdSe nanocrystallites into three-dimensional quantum dot superlattices. Science 270:1335–1338. doi:10.1126/science.270.5240.1335

Murray CB, Sun SH, Gaschler W, Doyle H, Betley TA, Kagan CR (2001) Colloidal synthesis of nanocrystals and nanocrystal superlattices. IBM J Res Dev 45:47–56

Nag BR (2000) Physics of quantum well devices. Kluwer Academic Publishers, Dordrecht, pp 105

Niemeyer CM (2003) Functional hybrid devices of proteins and inorganic nanoparticles. Angew Chem Int Ed 42:5796–5800. doi:10.1002/anie.200301703

Sapra S, Nanda J, Sarma DD, Abed el-al F, Hodes G (2001) Blue emission from cysteine ester passivated cadmium sulfide nanoclusters. Chem Commun (Camb) 2188–2189. doi:10.1039/b106420g

Sone ED, Stupp SI (2004) Semiconductor-encapsulated peptide-amphiphile nanofibers. J Am Chem Soc 126:12756–12757. doi:10.1021/ja0499344

Vossmeyer T, Katsikas L, Giersig M, Popovic IG, Diesner K, Chemseddine A, Eychmuller A, Weller H (1994) CdS nanoclusters: synthesis, characterization, size dependent oscillator strength, temperature shift of the excitonic transition energy, and reversible absorbance shift. J Phys Chem 98:7665–7673. doi:10.1021/j100082a044

Wang CW, Moffitt MG (2004) Surface-tunable photoluminescence from block copolymer-stabilized cadmium sulfide quantum dots. Langmuir 20:11784–11796. doi:10.1021/la048390g

Wang CW, Moffitt MG (2005) Nonlithographic hierarchical patterning of semiconducting nanoparticles via polymer/polymer phase separation. Chem Mater 17:3871–3878. doi:10.1021/cm0506252

Xue PC, Lu R, Huang Y, Jin M, Tan CH, Bao CY, Wang ZM, Zhao YY (2004) Novel pearl-necklace porous CdS nanofiber templated by organogel. Langmuir 20:6470–6475. doi:10.1021/la0493520

Zhang YH, Chen YM, Niu HJ, Gao MY (2006) Formation of CdS nanoparticle necklaces with functionalized dendronized polymers. Small 2:1314–1319. doi:10.1002/smll.200600067

Zhou Y, Ji QM, Masuda M, Kamiya S, Shimizu T (2006) Helical arrays of CdS nanoparticles tracing on a functionalized chiral template of glycolipid nanotubes. Chem Mater 18:403–406. doi:10.1021/cm051928z

Zimnitsky D, Jiang CY, Xu J, Lin ZQ, Tsukruk VV (2007) Substrate- and time-dependent photoluminescence of quantum dots inside the ultrathin polymer LbL film. Langmuir 23:4509–4515. doi:10.1021/la0636917